ACS OMEGA

Open Access

http://pubs.acs.org/journal/acsodf

Article

Raman Spectroscopy for the Quantitative Analysis of Solid Dosage Forms of the Active Pharmaceutical Ingredient of Febuxostat

Gull Rimsha,[‖] Muhammad Shahbaz,[‖] Muhammad Irfan Majeed,[*] Haq Nawaz,[*] Nosheen Rashid, Muhammad Waseem Akram, Ifra Shabbir, Kiran Kainat, Aiman Amir, Eiman Sultan, Mulja Munir, and Muhammad Imran

Cite This: *ACS Omega* 2023, 8, 41451−41457

Read Online

ACCESS | Metrics & More | Article Recommendations | Supporting Information

ABSTRACT: Raman spectroscopy has been used to characterize and quantify the solid dosage forms of the commercially available drug febuxostat. For this purpose, different formulations consisting of the febuxostat (API) and excipients with different concentrations of the API are prepared and analyzed by Raman spectroscopy to identify different spectral features related to the febuxostat API and excipients. Multivariate data analysis tools such as principal component analysis (PCA) and partial least-squares regression (PLSR) analysis are used for qualitative and quantitative analyses. PCA has been found to be useful for the qualitative monitoring of various solid dosage forms. PLSR analysis has led to the successful prediction of API concentration in the unknown samples with a sensitivity and a selectivity of 98 and 99%, respectively. Moreover, the root-mean-square error (RMSE) of calibration and validation of the PLSR model has been found to be 2.9033 and 1.35, respectively. Notably, it is found to be very helpful for the comparison between the self-made formulations of febuxostat and commercially available febuxostat tablets (40 and 80 mg) of two different brands (Gouric and Zurig). These results showed that Raman spectroscopy can be a useful and reliable technique for identifying and quantifying the active pharmaceutical ingredient (API) in commercially available solid dosage forms.

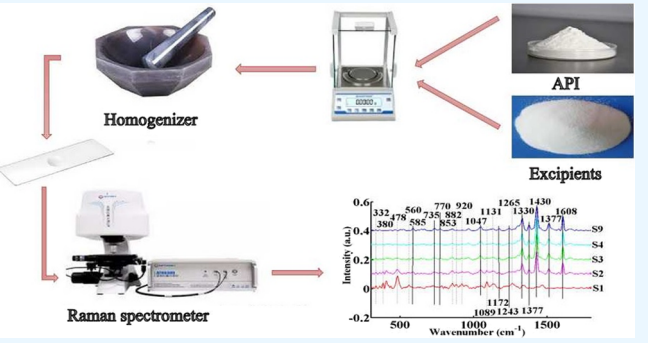

1. INTRODUCTION

Febuxostat is commercially used to treat hyperuricemia, including gout in the persistent stage, and is sold under the brand names *Adenuric* and *Uloric*. This drug was approved by the European Commission,[1] and in recent years, the FDA granted the use of febuxostat for the treatment of main kidney complications, chronic gout, and hyperuricemia for patients that do not have enough response regarding allopurinol.[2] Febuxostat blocks both its oxidized and reduced forms of xanthine oxidoreductase, which is essential for the conversion of xanthine into uric acid.[3] This can lead to control and lower the production of uric acid,[4] which causes an acute form of arthritis gout.

Various analytical techniques for determining the solid dosage forms of febuxostat have been reported, which include high-pressure liquid chromatography (HPLC),[5] ultraviolet spectrophotometric methods,[6] liquid chromatography, mass spectrometry,[7] and HPTLC,[8] in which toluene and methanol are used as a mobile phase and a large amount of sample is required. Mass spectrometry (MS) and nuclear magnetic resonance (NMR) spectroscopy are generally employed in the pharmaceutical research field. Although these methods are precise and reliable in solid dosage determination of febuxostat,[9] but running cost of these techniques is high. Raman spectroscopy has been employed for various analytical applications such as disease diagnosis,[10] screening of dengue infection,[11] characterization of different essential oils,[12] characterization of exopolysaccharides,[13] and characterization of organometallic complex formation.[14] Raman spectroscopy provides three main advantages over traditional techniques in solid dosage formulations. First, Raman spectroscopy is able to get a spectrum even when a sample is present within a sealed translucent container. Second, there is very little or no need for sample preparation, as the pharmaceutically active material is separated as crystalline salts. Third, coupling with an optical microscope study of minute particles in homogeneous solid-state matrices is possible.[15] Due to the benefits of Raman spectroscopy, this technique is most widely employed as an analytical tool in the recognition, characterization, and

Received: July 20, 2023
Revised: October 9, 2023
Accepted: October 11, 2023
Published: October 27, 2023

exploration of formulated pharmaceutical products.[16] Notably, regarding the use of HPLC for the samples having low concentrations of an analyte, such as febuxostat,[17] sitagliptin,[18] and cefixime,[19] another modality of Raman spectroscopy called surface-enhanced Raman spectroscopy (SERS) can be employed." Raman spectroscopy has previously been used to characterize pharmaceutical drugs such as sitagliptin,[20] cefixime,[21] losartan potassium,[22] ciprofloxacin,[23] paracetamol,[24] and ampicillin[25] in both qualitative and quantitative ways.

In this study, solid dosage formulations of febuxostat API (Figure 1) are being characterized using Raman spectroscopy,

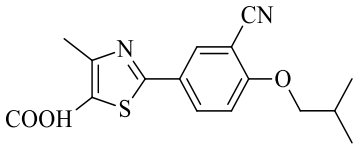

Figure 1. Chemical structure of febuxostat.

and it is found that there is no such study published yet. Different formulations of the febuxostat API are made by mixing the API and excipients in varied quantities. For qualitative analysis, principal component analysis (PCA) is employed for these drug formulations, which differentiates the different samples of API using spectral changes with an increase in the concentration of API. For quantitative analysis, partial least-squares regression analysis (PLSR) is being investigated for the determination of the concentration of self-made unknown/blind febuxostat samples.

2. RESULTS AND DISCUSSION

2.1. Mean Raman Spectra of Febuxostat Samples. Figure 2 represents the mean Raman spectra of various

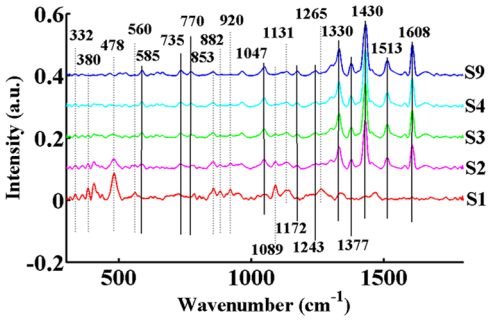

Figure 2. Mean Raman spectra of febuxostat with five different formulations S1: pure excipients, S2−S4: different concentrations of the API, and excipients S9: pure febuxostat API.

pharmaceutical samples, including the pure active pharmaceutical ingredient (API) of febuxostat (S9), pure excipients (S1), and seven different concentrations of API combined with excipients (S2 to S8). Raman spectral features associated with febuxostat API and those associated with excipients are labeled with dotted lines, while the most significant differences are represented by vertical solid lines. Table 1 lists the peak assignments of these differentiated spectral features along with the relevant references from the literature. The Raman spectral features of different febuxostat formulations are associated with an increase in API concentration and a decrease in excipient concentration. It is concluded from the mean Raman plot that

Table 1. Details of Raman Spectral Peaks Found in the Spectral Data of Different Samples of the Febuxostat API

wavenumber (cm^{-1})	peak assignments	references
332	NCC in-plane def.	26
380	starch str.	27
478	titanium bend	27
560	CO_2 rock vib. mode	28
585	OH out-of-plane bend	20
735	CS str. due to thiazole bands	29
770	C−H and C−CN out-of-plane bend	30
853	δ(CCH) in the aromatic ring	31
882	C−C str., CH_2 rock	32
920	CNC in-plane def.	33
1243	CH_2 wag, C−N str.	34
1047	C−O−C asym. and sym. str. vib.	35
1089	C−O str. and CH_3 rock	32
1131	C−N str.	36
1172	str. modes of aromatic benzene	37
1265	C−N str. vib. in amide	38
1330	C−N str. and imidazole ring str.	39
1377	C−N str. in the amide group	40
1430	CH_3 sci.	41
1513	C═C str. vib. of the phenyl ring	42
1608	C═O str, ν(C═N) azomethine	21,43

as the febuxostat API concentration in solid dosage forms increases, the intensity of different features goes on increasing.

The Raman features associated with API have been observed at 1513 and 1608 cm^{-1} because of the stretching vibrations of C═O and ν(C═N) in the azomethine group and showed an increase in intensity as the concentration of API increases. Raman spectral features observed at 1430 and 1377 cm^{-1} are due to scissoring vibration in the CH_3 group and C−N stretching vibration in the amide group. Characteristics Raman peaks at 1330, 1243, and 1265 cm^{-1} are assigned to CN stretching vibrations and CH_2 wagging vibrations in the amide group, while the peak at 1172 cm^{-1} represents the benzene stretching modes. The stretching vibrations in the C−O−C group, which are symmetric and asymmetric, enable the identification of a strong Raman feature at 1047 cm^{-1}. Furthermore, two Raman peaks were observed at 1330 and 770 cm^{-1} due to the stretching modes of the benzene ring and the out-of-plane bending of C−H and C−CN. Another distinguished Raman feature observed at 735 cm^{-1} is assigned to CS stretching due to thiazole bands. The Raman spectral features associated with excipients can be observed in the mean Raman plot (Figure 2) at 478 and 560 cm^{-1} due to titanium bending and rocking vibration modes of CO_2, respectively. Some characteristic Raman features of excipients have been observed at 332 and 380 cm^{-1} because of in-plane deformation of NCC and stretching vibration in starch, respectively. The Raman peaks at 853, 882, and 920 cm^{-1}, respectively, represent the vibration of the aromatic ring, C−C stretching and CH_2 rocking, and CNC in-plane deformation. The CH_3 rocking and C−N stretching vibrations, which are attributed to excipients, are represented by the most prominent Raman features, indicating highly intense peaks at 1089 and 1131 cm^{-1}.

2.2. Principal Component Analysis (PCA). PCA is used to perform the qualitative analysis of Raman spectral data sets of different formulations of febuxostat API with different concentrations of excipients. In order to identify changes in

https://doi.org/10.1021/acsomega.3c05243
ACS Omega 2023, 8, 41451−41457

spectral features that occur in various formulations of febuxostat as a result of an increase in API concentration and a decrease in excipient concentration, this multivariate data analysis technique is used to clarify the variability in Raman spectral data sets. The PCA scatter plot of samples (S1 to S9) clearly differentiates the Raman spectral data sets of the samples in the form of clusters, as shown in Figure 3.

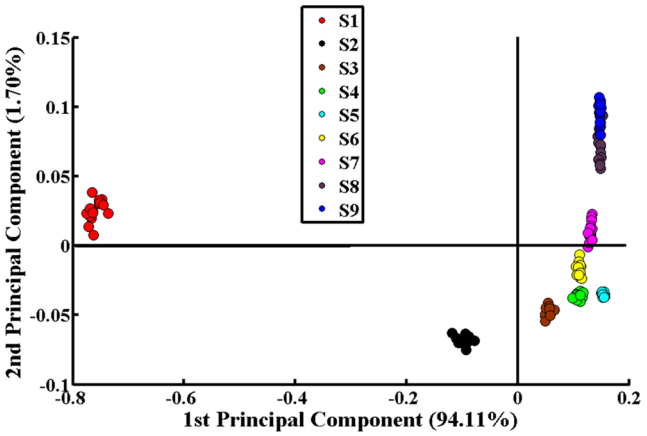

Figure 3. PCA scatter plot of Raman spectral data for the solid dosage forms of febuxostat (S1−S9).

To confirm the Raman spectral features shown in Figure 2, pairwise PCA is carried out on Raman spectral data sets of pure excipients (S1) and the pure febuxostat API. As can be seen, PC-1 explains 94.11% of the variability in the spectral data sets, while PC-2 explains 1.70%. (S9). These results are presented in the PCA scatter plot (Figure 4(a)) and PCA loadings (Figure 4(b)).

Raman spectral data for pure excipients (S1) are clustered along the PC-1 negative axis, whereas data for the pure febuxostat API (S9) are clustered along the positive axis. The negative and positive loadings in Figure 4(b) are the spectral features responsible for this differentiation. The Raman features identified as positive PC-1 loadings, which are associated with the pure API, are found to be at 585 cm^{-1} (out-of-plane bending of the carboxylic OH group), 735 cm^{-1} (CS stretching due to thiazole bands), 770 cm^{-1} (out-of-plane bending of C−CN and C−H), 1047 cm^{-1} (stretching vibration of C−O−C with symmetric and asymmetric modes), 1172 cm^{-1} (stretching vibration of the aromatic benzene ring), 1243 cm^{-1} (CH_2 wagging, C−N stretching), 1330 cm^{-1} (CN stretching vibration), 1377 cm^{-1} (amide C−N stretching vibration), 1430 cm^{-1} (CH_3 scissoring vibration), 1513 cm^{-1} (phenyl ring stretching vibration of C═C), and 1608 cm^{-1} (stretching C═O, ν(C═N) stretching in the azomethine group).

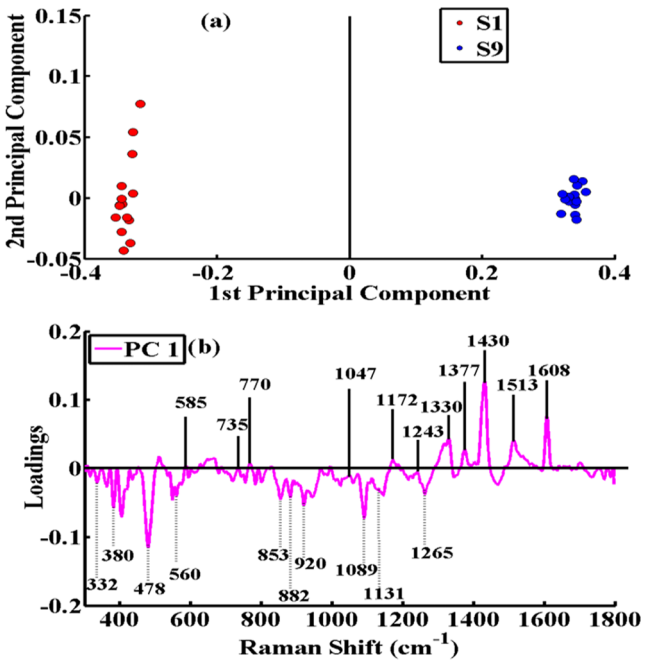

Figure 4. Pairwise PCA scatter plot (a) and PCA loadings (b) are used to display the Raman spectral data of pure excipients (S1) and the pure febuxostat API (S9).

The negative loadings represent the Raman features of excipients with dotted lines observed at 332 cm^{-1} (in-plane deformation of NCC), 380 cm^{-1} (stretching vibration in starch), 478 cm^{-1} (bending vibrations in titanium), 560 cm^{-1} (CO_2 rocking vibration mode), 853 cm^{-1} (bending δ(CCH) in the aromatic ring), 882 cm^{-1} (C−C stretching, CH_2 rocking), 920 cm^{-1} (CNC in-plane deformation), 1089 cm^{-1} (C−O stretching and CH3 rocking), 1131 cm^{-1} (stretching vibration of C−N), and 1265 cm^{-1}(stretching vibration of C−N in amide). These results demonstrate that PCA can distinguish the active pharmaceutical ingredient (API) from excipients based on Raman spectral features.

PCA analysis has major advantages as it removes the correlated features, reduces overfitting, and improves visualization.[44] Regarding its disadvantages, PCA is not robust with respect to missing values, which means that if the data have gaps or errors, this data analysis tool may not work properly or produce inaccurate results. In order to confirm the analysis capability and efficiency of PCA for the Raman spectral data sets used in the current study, another multivariate data analysis technique called PLSR is employed. This analysis explains the maximum variability in the response within the context of linear regression.[45] PLSR models can be prone to overfitting, especially when the number of latent variables/components is not properly chosen.[46] To overcome this issue, the number of latent variables/components required to build the PLSR model is carefully chosen, as indicated in Figure 5.

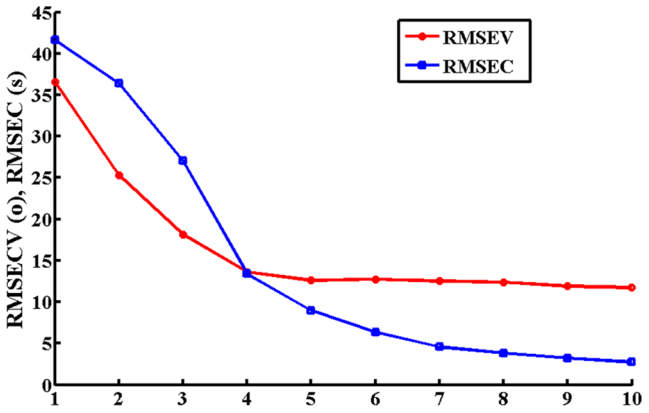

Figure 5. Optimal number of latent variables (LV) for PLSR model development for Raman spectral data sets of various formulations of the febuxostat API.

https://doi.org/10.1021/acsomega.3c05243
ACS Omega 2023, 8, 41451−41457

2.3. Partial Least-Squares Regression Analysis (PLSR).

The potential of Raman spectroscopy to predict the concentration of the API in blind pharmaceutical samples was investigated by using a PLSR model of Raman spectral data collected from various concentrations of febuxostat. The Raman spectral data of febuxostat with nine different formulations/concentrations were assembled in a matrix and excluded from the sample from which the model's performance was assessed as an unknown concentration. To evaluate the efficiency of the developed model, other febuxostat formulations also taken as unknown/blind samples are given in Table 2. After the predictive model has been established, it can be helpful in evaluating and monitoring the different unknown concentrations of febuxostat.

Table 2. Details of Some Unknown Febuxostat Samples Randomly Selected to Evaluate the Demonstration of a PLS Regression Model for Predicting API Concentrations

sample names	measured concentration	predicted concentration	R^2	RMSEC	RMSEV
S2	20 mg	21.45 mg	0.98760	2.6702	1.45
S3	40 mg	41.63 mg	0.99708	0.7665	1.63
S4	60 mg	58.65 mg	0.99878	2.9033	1.35
S5	80 mg	79.23 mg	0.99910	0.8454	0.77
S6	100 mg	101.1 mg	0.99908	1.9809	1.10
S8	140 mg	142.03 mg	0.98607	2.4701	2.03

The complexity of the optimal model was determined by using cross-validation with calibration. This process involves the calibration data set to select the optimal number of LV and cross-validation to evaluate the developed PLSR model. Notably, four latent variables (LVs) were selected for developing this predictive model, which provides the lowest root-mean-square error, as given in Figure 5. The root-mean-square error of calibration (RMSEC) is 2.9033 mg and the reliability of this calibration (R^2) is 0.99%, which is shown by the PLSR calibration model in Figure 6(A).

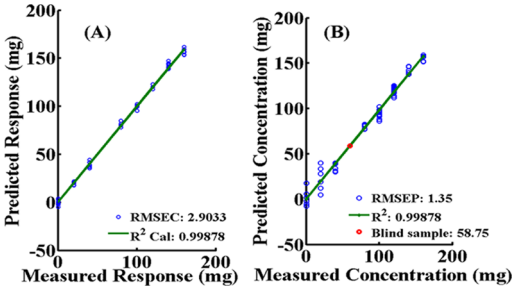

Figure 6. Demonstration of a calibration set (A) and a prediction set (B) of the partial least-squares regression (PLSR) model for quantifying a self-made blind febuxostat sample (S4).

These values clearly indicate the reliability of the PLSR model for the calibration of Raman data sets representing different drug (febuxostat) concentrations based on the response of Raman spectroscopy. The PLSR validation model was used to predict the unknown concentration of febuxostat S4 and randomly selected other formulations as unknown/blind samples. The unknown sample (S4) having an actual concentration of API as 60 mg, as shown in Figure 6(B), was predicted by the PLSR model as 58.65 mg. The root-mean-square error of cross-validation (RMSEP) is observed as 1.35 mg, and the reliability of the validation model is found to be 0.99%.

The PLSR model is also built to compare different prepared febuxostat formulations with the commercially available standard formulations of febuxostat (40 and 80 mg) of two different brands (Gouric and Zurig). This built PLSR model showed 99% accuracy, sensitivity, and specificity in unknown samples' (febuxostat) concentration prediction as compared with that of standard samples (febuxostat). Figures 7 and 8 show the demonstration of the calibration set and the prediction set of the PLSR model for commercially available febuxostat of 40 and 80 mg (Gouric brand) as a blind sample.

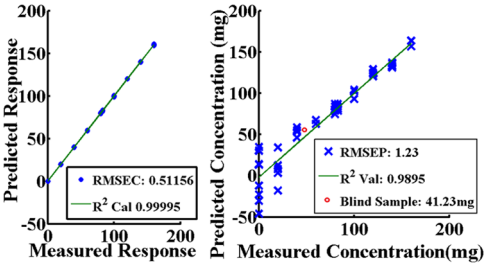

Figure 7. Demonstration of a calibration set and a prediction set of the PLSR model for quantification of commercially available febuxostat of 40 mg (Gouric brand) as a blind sample.

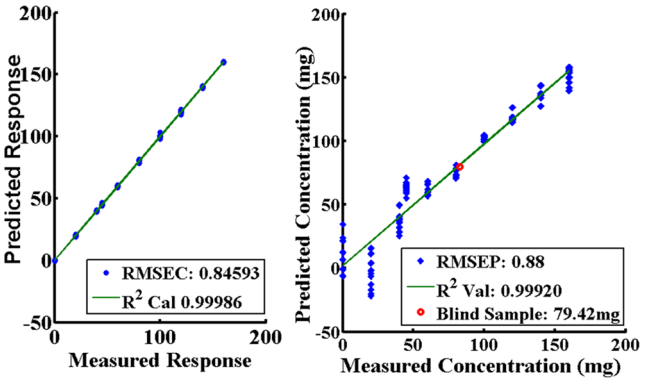

Figure 8. Demonstration of a calibration set and a prediction set of the PLSR model for quantification of commercially available febuxostat of 80 mg (Gouric brand) as a blind sample.

2.4. Coefficients of Regression Analysis.

As shown in Figure 9, the PLSR regression coefficients indicate the presence of Raman spectral features associated with API

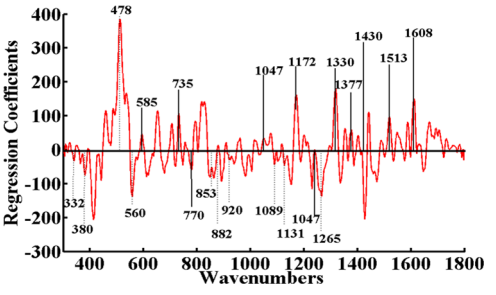

Figure 9. Raman spectral data sets for different formulations of febuxostat API (S1−S9) from the regression coefficients of the PLSR model.

https://doi.org/10.1021/acsomega.3c05243
ACS Omega 2023, 8, 41451−41457

(febuxostat) and excipients. The regression coefficients associated with API are observed at 585 cm^{-1} (out-of-plane bending of the carboxylic OH group), 735 cm^{-1} (CS stretching due to thiazole bands), 770 cm^{-1} (out-of-plane bending of C−CN and C−H), 1047 cm^{-1} (stretching vibration of C−O−C with symmetric and asymmetric modes), 1172 cm^{-1} (stretching vibration of the aromatic benzene ring), 1243 cm^{-1} (CH_2 wagging, C−N stretching), 1330 cm^{-1} (C−N stretching vibration), 1377 cm^{-1} (amide C−N stretching vibration), 1430 cm^{-1} (CH_3 scissoring vibration), 1513 cm^{-1} (phenyl ring stretching vibration of C═C), and 1608 cm^{-1} (C═O stretching, ν(C═N) in the azomethine group). The regression coefficients associated with excipients are observed at 332 cm^{-1} (in-plane deformation of NCC), 380 cm^{-1} (stretching vibration in starch), and 478 cm^{-1} (bending vibrations in titanium). The Raman spectral features in the mean Raman spectra of various formulations of febuxostat API are identical to the regression coefficients of the PLSR model (Figure 2).

3. CONCLUSIONS

In this study, solid dosage analysis of different formulations of febuxostat API has been carried out using Raman spectroscopy and different multivariate data analysis techniques such as the PCA and PLSR models. For this purpose, various spectral features associated with febuxostat API are identified and used for both qualitative and quantitative analyses. The quantitative analysis of the blind sample was also done by use of partial least-squares regression analysis to test the performance of the PLSR prediction model. This analytical method has the potential to be employed in the pharmaceutical sector.

4. MATERIALS AND METHODS

4.1. Sample Preparation. Febuxostat API was obtained from Fynk Pharmaceuticals (Pvt.) (Lahore, Pakistan) and was used as a reference standard. Different concentrations of excipients and API were mixed in milligrams to form different formulations, as shown in Table 3. Different pharmaceutical formulations were made by mixing of API of febuxostat and different excipients, including talcum powder, magnesium, titanium, starch, and lactose, in an equal ratio, followed by their homogenization using a pestle mortar.

Table 3. Details of Nine Febuxostat Samples That Were Made by Mixing different Concentrations of API and Excipients

sample name	API (mg)	excipients (mg)	total weight (mg)
S1	0	160	160
S2	20	140	160
S3	40	120	160
S4	60	100	160
S5	80	80	160
S6	100	60	160
S7	120	40	160
S8	140	20	160
S9	160	0	160

4.2. Raman Spectral Acquisition. Raman spectral measurements for each febuxostat sample in powder form were performed by using a Raman spectrometer (ATR8300BS Optosky, China). From each febuxostat sample, by placing each sample on the aluminum slide, 15 Raman spectra were collected. For this, a 40 mW 785 nm laser was shed on the sample with the help of a 40X objective lens and an acquisition time of 10 s to acquire Raman spectra in the wavenumber range of 300−1800 cm^{-1}.

4.3. Data Preprocessing. To preprocess the Raman spectral data, MatLab version 7.8.0.347 and an established set of protocols were used for all of the febuxostat samples. Preprocessing included the steps of smoothing, vector normalization, baseline correction, and substrate removal. The contribution of the substrate (aluminum slide) was subtracted from the spectral data sets, and the spectra were smoothed using the Savitzky−Golay method in three 15-point windows. Savitzky−Golay smoothing filters are used to remove noise from a signal. The rubber band correction was used to adjust the baseline of the raw Raman spectra. Baseline correction is a significant preprocessing method used to distinguish the true spectroscopic signals and remove background noise. Notably, the intensity-to-concentration relationship in the spectral data was preserved by vector normalization of the spectra for the PCA qualitative analysis but not for the PLSR quantitative analysis.

4.4. Data Analysis. The Raman spectral data of different samples of febuxostat are analyzed by calculating their respective mean spectra. Table 1 shows how the results were interpreted using Raman spectral feature assignments from the literature. Different samples of febuxostat with varying API concentrations were classified using PCA. Principal component analysis (PCA) is a statistical method that converts the correlated variables into a smaller set of uncorrelated variables known as principal components, thereby reducing the dimensionality of data while maintaining variability (PCs).[47] The first principal component accounts for the predominant source of data variability, the second principal component accounts for the second-highest source of the remaining variability, and so on.

The PC loadings can be seen as an orthogonal dimension that enables the differentiation of different classes of spectral data based on their coefficients because each spectrum of different febuxostat formulations scores along these dimensions.[48] Partial least-squares regression is used to analyze the covariance of Raman spectral data (x-variables) and known concentrations (y-variables) to perform the quantitative analysis of different formulations of the API of febuxostat. A regression model was developed based on how the Raman spectral characteristics of febuxostat API changed as the percentage weight of API in different formulations increased. The validity of this predictive PLS regression model is evaluated using cross-validation and root-mean-square error of calibration (RMSECV). Through the use of leave-one sample (15 spectra) out cross-validation, the optimal number of latent variables (LVs) is required to develop a reliable model that avoids overfitting, and this method was used to ensure that the PLSR analysis was not biased because all spectra obtained from a formulation were included in either the calibration or test data sets.

■ ASSOCIATED CONTENT

Supporting Information

The Supporting Information is available free of charge at https://pubs.acs.org/doi/10.1021/acsomega.3c05243.

PCA scatter plot, mean Raman spectra, and PLSR model details of two commercial drugs (PDF)

https://doi.org/10.1021/acsomega.3c05243
ACS Omega 2023, 8, 41451−41457

AUTHOR INFORMATION

Corresponding Authors

Muhammad Irfan Majeed − *Department of Chemistry, University of Agriculture Faisalabad, Faisalabad 38000, Pakistan;* orcid.org/0000-0003-0506-6060; Email: irfan.majeed@uaf.edu.pk

Haq Nawaz − *Department of Chemistry, University of Agriculture Faisalabad, Faisalabad 38000, Pakistan;* orcid.org/0000-0003-2739-4735; Email: haqchemist@yahoo.com

Authors

Gull Rimsha − *Department of Chemistry, University of Agriculture Faisalabad, Faisalabad 38000, Pakistan*

Muhammad Shahbaz − *Department of Chemistry, University of Agriculture Faisalabad, Faisalabad 38000, Pakistan*

Nosheen Rashid − *Department of Chemistry, University of Education, Faisalabad Campus, Faisalabad 38000, Pakistan*

Muhammad Waseem Akram − *Department of Chemistry, University of Agriculture Faisalabad, Faisalabad 38000, Pakistan*

Ifra Shabbir − *Department of Chemistry, University of Agriculture Faisalabad, Faisalabad 38000, Pakistan*

Kiran Kainat − *Department of Chemistry, University of Agriculture Faisalabad, Faisalabad 38000, Pakistan*

Aiman Amir − *Department of Chemistry, University of Agriculture Faisalabad, Faisalabad 38000, Pakistan*

Eiman Sultan − *Department of Chemistry, University of Agriculture Faisalabad, Faisalabad 38000, Pakistan*

Mulja Munir − *Department of Chemistry, University of Agriculture Faisalabad, Faisalabad 38000, Pakistan*

Muhammad Imran − *Department of Chemistry, Faculty of Science, King Khalid University, Abha 61413, Saudi Arabia*

Complete contact information is available at: https://pubs.acs.org/10.1021/acsomega.3c05243

Author Contributions

‖G.R. and M.S. contributed equally to this work.

Notes

The authors declare no competing financial interest.

ACKNOWLEDGMENTS

M. Imran expresses his appreciation to the Deanship of Scientific Research at King Khalid University, Saudi Arabia, for funding this work through a research program under grant number R.G.P. 2/522/44.

REFERENCES

(1) Hu, M.; Tomlinson, B. Febuxostat in the management of hyperuricemia and chronic gout: a review. *Ther. Clin. Risk Manage.* **2008**, *4* (6), 1209 DOI: 10.2147/tcrm.s3310.

(2) Stamp, L.; O'Donnell, J.; Chapman, P. Emerging therapies in the long-term management of hyperuricaemia and gout. *Intern. Med. J.* **2007**, *37* (4), 258−266.

(3) Nishino, T.; Okamoto, K. Mechanistic insights into xanthine oxidoreductase from development studies of candidate drugs to treat hyperuricemia and gout. *JBIC, J. Biol. Inorg. Chem.* **2015**, *20* (2), 195−207.

(4) Dawson, J.; Quinn, T.; Walters, M. Uric acid reduction: a new paradigm in the management of cardiovascular risk? *Curr. Med. Chem.* **2007**, *14* (17), 1879−1886, DOI: 10.2174/092986707781058797.

(5) Vaibhav, S.; Mohit, M.; Sadhana, R. Validation of RP-HPLC for simultaneous estimation of febuxostat and diclofenac potassium in bulk drug and in bilayer tablet formulation. *Int. Res. J. Pharm.* **2013**, *4*, 103−106, DOI: 10.7897/2230-8407.04921.

(6) Liyun, Z.; Gengliang, Y.; Youlan, P. Dissolution determination of Febuxostat tablets by UV spectrophotography. *J. Hebei Med. Coll. Contin. Educ.* **2010**, *27* (5), 8−10, DOI: 10.3969/j.issn.1674-490X.2010.05.003.

(7) Kadivar, M. H.; Sinha, P. K.; Kushwah, D.; Jana, P.; Sharma, H.; Bapodra, A. Study of impurity carryover and impurity profile in Febuxostat drug substance by LC−MS/MS technique. *J. Pharm. Biomed. Anal.* **2011**, *56* (4), 749−757.

(8) Sunitha, P. G.; Ilango, K. Validated RP-HPLC and HPTLC methods for simultaneous estimation of febuxostat and diclofenac sodium in pharmaceutical dosage form. *Eur. J. Chem.* **2014**, *5* (3), 545−549.

(9) Liu, G.-k.; Zheng, H.; Lu, J.-l. Recent progress and perspective of trace antibiotics detection in aquatic environment by surface-enhanced Raman spectroscopy. *Trends Environ. Anal. Chem.* **2017**, *16*, 16−23.

(10) Ryzhikova, E.; Ralbovsky, N. M.; Sikirzhytski, V.; Kazakov, O.; Halamkova, L.; Quinn, J.; Zimmerman, E. A.; Lednev, I. K. Raman spectroscopy and machine learning for biomedical applications: Alzheimer's disease diagnosis based on the analysis of cerebrospinal fluid. *Spectrochim. Acta, Part A* **2021**, *248*, No. 119188.

(11) Mahmood, T.; Nawaz, H.; Ditta, A.; Majeed, M.; Hanif, M.; Rashid, N.; Bhatti, H.; Nargis, H.; Saleem, M.; Bonnier, F. Raman spectral analysis for rapid screening of dengue infection. *Spectrochim. Acta, Part A* **2018**, *200*, 136−142, DOI: 10.1016/j.saa.2018.04.018.

(12) Nawaz, H.; Hanif, M. A.; Ayub, M. A.; Ishtiaq, F.; Kanwal, N.; Rashid, N.; Saleem, M.; Ahmad, M. Raman spectroscopy for the evaluation of the effects of different concentrations of Copper on the chemical composition and biological activity of basil essential oil. *Spectrochim. Acta, Part A* **2017**, *185*, 130−138.

(13) Tahir, M.; Majeed, M. I.; Nawaz, H.; Ali, S.; Rashid, N.; Kashif, M.; Ashfaq, I.; Ahmad, W.; Ghauri, K.; Sattar, F. Raman spectroscopy for the analysis of different exo-polysaccharides produced by bacteria. *Spectrochim. Acta, Part A* **2020**, *237*, No. 118408, DOI: 10.1016/j.saa.2020.118408.

(14) Ashraf, M. N.; Majeed, M. I.; Nawaz, H.; Iqbal, M. A.; Iqbal, J.; Iqbal, N.; Hasan, A.; Rashid, N.; Abubakar, M.; Nawaz, M. Z. Raman spectroscopic characterization of selenium N-heterocyclic carbene compounds. *Spectrochim. Acta, Part A* **2022**, *270*, No. 120823, DOI: 10.1016/j.saa.2021.120823.

(15) Chan, K.; Fleming, O.; Kazarian, S.; Vassou, D.; Chryssikos, G. D.; Gionis, V. Polymorphism and devitrification of nifedipine under controlled humidity: a combined FT-Raman, IR and Raman microscopic investigation. *J. Raman Spectrosc.* **2004**, *35* (5), 353−359.

(16) Bell, S. E.; Beattie, J. R.; McGarvey, J. J.; Peters, K. L.; Sirimuthu, N.; Speers, S. J. Development of sampling methods for Raman analysis of solid dosage forms of therapeutic and illicit drugs. *J. Raman Spectrosc.* **2004**, *35* (5), 409−417.

(17) Magdy, G.; Abdel Hakiem, A. F.; Belal, F.; Abdel-Megied, A. M. A novel quality by design approach for development and validation of a green reversed-phase HPLC method with fluorescence detection for the simultaneous determination of lesinurad, febuxostat, and diflunisal: application to human plasma. *J. Sep. Sci.* **2021**, *44* (11), 2177−2188.

(18) Rezaee, R.; Qomi, M.; Piroozi, F. Hollow-fiber micro-extraction combined with HPLC for the determination of sitagliptin in urine samples. *J. Serb. Chem. Soc.* **2015**, *80* (10), 1311−1320, DOI: 10.2298/JSC141227046R.

(19) Attimarad, M. V.; Alnajjar, A. O. A conventional HPLC-MS method for the simultaneous determination of ofloxacin and cefixime in plasma: Development and validation. *J. Basic Clin. Pharm.* **2013**, *4* (2), 36−41, DOI: 10.4103/0976-0105.113606.

(20) Bakkar, M. A.; Nawaz, H.; Majeed, M. I.; Naseem, A.; Ditta, A.; Rashid, N.; Ali, S.; Bajwa, J.; Bashir, S.; Ahmad, S. Raman spectroscopy for the qualitative and quantitative analysis of solid dosage forms of Sitagliptin. *Spectrochim. Acta, Part A* **2021**, *245*, No. 118900, DOI: 10.1016/j.saa.2020.118900.

(21) Bajwa, J.; Nawaz, H.; Majeed, M. I.; Hussain, A. I.; Farooq, S.; Rashid, N.; Bakkar, M. A.; Ahmad, S.; Hyat, H.; Bashir, S. Quantitative analysis of solid dosage forms of cefixime using Raman spectroscopy. *Spectrochim. Acta, Part A* **2020**, *238*, No. 118446, DOI: 10.1016/j.saa.2020.118446.
(22) Shafaq, S.; Majeed, M. I.; Nawaz, H.; Rashid, N.; Akram, M.; Yaqoob, N.; Tariq, A.; Shakeel, S.; ul Haq, A.; Saleem, M. Quantitative analysis of solid dosage forms of Losartan potassium by Raman spectroscopy. *Spectrochim. Acta, Part A* **2022**, *272*, No. 120996, DOI: 10.1016/j.saa.2022.120996.
(23) Assi, S.; Watt, R. A.; Moffat, A. C. On the quantification of ciprofloxacin in proprietary Ciproxin tablets and generic ciprofloxacin tablets using handheld Raman spectroscopy. *J. Raman Spectrosc.* **2012**, *43* (8), 1049−1057.
(24) Lakhwani, G. R.; Sherikar, O.; Mehta, P. J. Nondestructive and rapid concurrent estimation of paracetamol and nimesulide in their combined dosage form using raman spectroscopic technique. *Indian J. Pharm. Sci.* **2013**, *75* (2), 211−216.
(25) Baraldi, C.; Tinti, A.; Ottani, S.; Gamberini, M. C. Characterization of polymorphic ampicillin forms. *J. Pharm. Biomed. Anal.* **2014**, *100*, 329−340.
(26) Lima, J., Jr; Freire, P.; Lima, R.; Moreno, A.; Mendes Filho, J.; Melo, F. Raman scattering of L-valine crystals. *J. Raman Spectrosc.* **2005**, *36* (11), 1076−1081, DOI: 10.1002/jrs.1410.
(27) De Veij, M.; Vandenabeele, P.; De Beer, T.; Remon, J. P.; Moens, L. Reference database of Raman spectra of pharmaceutical excipients. *J. Raman Spectrosc.* **2009**, *40* (3), 297−307.
(28) Tsiachris, D.; Tsioufis, C.; Mazzone, P.; Katsiki, N.; Stefanadis, C. Atrial fibrillation and chronic kidney disease in hypertension: a common and dangerous triad. *Curr. Vasc. Pharmacol.* **2015**, *13* (1), 111−120.
(29) Miyazaki, J.; Takiyama, H.; Nakata, M. Isocyano compounds newly recognized in photochemical reaction of thiazole: matrix-isolation FT-IR and theoretical studies. *RSC Adv.* **2017**, *7* (9), 4960−4974.
(30) Bresson, S.; Marssi, El.; Khelifa, M.; Raman, B. Raman spectroscopy investigation of various saturated monoacid triglycerides. *Chem. Phys. Lipids* **2005**, *134* (2), 119−129, DOI: 10.1016/j.chemphyslip.2004.12.009.
(31) Edwards, H.; Farwell, D.; Newton, E.; Perez, F. R.; Villar, S. J. Application of FT-Raman spectroscopy to the characterisation of parchment and vellum, I; novel information for paleographic and historiated manuscript studies. *Spectrochim. Acta, Part A* **2001**, *57* (6), 1223−1234, DOI: 10.1016/S1386-1425(00)00467-4.
(32) Casari, C. S.; Bassi, A. L.; Baserga, A.; Ravagnan, L.; Piseri, P.; Lenardi, C.; Tommasini, M.; Milani, A.; Fazzi, D.; Bottani, C. E. Low-frequency modes in the Raman spectrum of s p− s p 2 nanostructured carbon. *Phys. Rev. B* **2008**, *77* (19), No. 195444, DOI: 10.1103/PhysRevB.77.195444.
(33) Cherepy, N. J.; Shreve, A. P.; Moore, L. J.; Franzen, S.; Boxer, S. G.; Mathies, R. A. Near-infrared resonance Raman spectroscopy of the special pair and the accessory bacteriochlorophylls in photosynthetic reaction centers. *J. Phys. Chem. A* **1994**, *98* (23), 6023−6029.
(34) Almond, L. M.; Hutchings, J.; Lloyd, G.; Barr, H.; Shepherd, N.; Day, J.; Stevens, O.; Sanders, S.; Wadley, M.; Stone, N. Endoscopic Raman spectroscopy enables objective diagnosis of dysplasia in Barrett's esophagus. *Gastrointest. Endoscopy* **2014**, *79* (1), 37−45, DOI: 10.1016/j.gie.2013.05.028.
(35) Lau, K.; Isabelle, M.; Lloyd, G. R.; Old, O.; Shepherd, N.; Bell, I. M.; Dorney, J.; Lewis, A.; Gaifulina, R.; Rodriguez-Justo, M. *The road map towards providing a robust Raman spectroscopy-based cancer diagnostic platform and integration into clinic*, Biomedical Vibrational Spectroscopy 2016: Advances in Research and Industry, SPIE201631-39.
(36) Keating, M. E.; Nawaz, H.; Bonnier, F.; Byrne, H. J. Multivariate statistical methodologies applied in biomedical Raman spectroscopy: assessing the validity of partial least squares regression using simulated model datasets. *Analyst* **2015**, *140* (7), 2482−2492.
(37) Shi, L.; Xiong, H.; Shen, Y.; Long, R.; Wei, L.; Min, W. Electronic resonant stimulated Raman scattering micro-spectroscopy. *J. Phys. Chem. B* **2018**, *122* (39), 9218−9224.
(38) Cheng, W. T.; Liu, M. T.; Liu, H. N.; Lin, S. Y. Micro-Raman spectroscopy used to identify and grade human skin pilomatrixoma. *Microsc. Res. Tech.* **2005**, *68* (2), 75−79.
(39) Wirges, M.; Müller, J.; Kása, P., Jr; Regdon, G., Jr; Pintye-Hódi, K.; Knop, K.; Kleinebudde, P. From Mini to Micro Scale—Feasibility of Raman Spectroscopy as a Process Analytical Tool (PAT). *Pharmaceutics* **2011**, *3* (4), 723−730.
(40) Liu, C.-H.; Zhou, Y.; Sun, Y.; Li, J.; Zhou, L.; Boydston-White, S.; Masilamani, V.; Zhu, K.; Pu, Y.; Alfano, R. Resonance Raman and Raman spectroscopy for breast cancer detection. *Technol. Cancer Res. Treat.* **2013**, *12* (4), 371−382, DOI: 10.7785/tcrt.2012.500325.
(41) Iliescu, T.; Baia, M.; Pavel, I. Raman and SERS investigations of potassium benzylpenicillin. *J. Raman Spectrosc.* **2006**, *37* (1−3), 318−325.
(42) Samyn, P.; Vancraenenbroeck, J.; Verpoort, F.; De Baets, P. The use of post-mortem Raman spectroscopy in explaining friction and wear behaviour of sintered polyimide at high temperature. *Tribotest* **2006**, *12* (3), 223−236.
(43) Koleva, B. B.; Kolev, T. M.; Spiteller, M. Determination of cephalosporins in solid binary mixtures by polarized IR-and Raman spectroscopy. *J. Pharm. Biomed. Anal.* **2008**, *48* (1), 201−204.
(44) Zebari, R.; Abdulazeez, A.; Zeebaree, D.; Zebari, D.; Saeed, J. A comprehensive review of dimensionality reduction techniques for feature selection and feature extraction. *J. Appl. Sci. Technol. Trends* **2020**, *1* (2), 56−70, DOI: 10.38094/jastt1224.
(45) Liu, C.; Zhang, X.; Nguyen, T. T.; Liu, J.; Wu, T.; Lee, E.; Tu, X. M. Partial least squares regression and principal component analysis: similarity and differences between two popular variable reduction approaches. *Gen. Psychiatry* **2022**, *35* (1), No. e100662, DOI: 10.1136/gpsych-2021-100662.
(46) González-Domínguez, R.; Sayago, A.; Fernández-Recamales, Á. An overview on the application of chemometrics tools in food authenticity and traceability. *Foods* **2022**, *11* (23), 3940.
(47) Saade, J.; Pacheco, M. T. T.; Rodrigues, M. R.; Silveira, L., Jr Identification of hepatitis C in human blood serum by near-infrared Raman spectroscopy. *Spectroscopy* **2008**, *22* (5), 387−395, DOI: 10.1155/2008/419783.
(48) Nawaz, H.; Rashid, N.; Saleem, M.; Asif Hanif, M.; Irfan Majeed, M.; Amin, I.; Iqbal, M.; Rahman, M.; Ibrahim, O.; Baig, S. Prediction of viral loads for diagnosis of Hepatitis C infection in human plasma samples using Raman spectroscopy coupled with partial least squares regression analysis. *J. Raman Spectrosc.* **2017**, *48* (5), 697−704, DOI: 10.1002/jrs.5108.

https://doi.org/10.1021/acsomega.3c05243
ACS Omega 2023, 8, 41451−41457